

Research Paper

# Quantitative analysis of the stabilization by substrate of *Staphylococcus aureus* PC1 $\beta$ -lactamase

Annabelle Lejeune <sup>a</sup>, Marc Vanhove <sup>a</sup>, Josette Lamotte-Brasseur <sup>a</sup>, Roger H. Pain <sup>b</sup>,  
Jean-Marie Frère <sup>a</sup>, André Matagne <sup>a, \*</sup>

<sup>a</sup>Laboratoire d'Enzymologie, Centre d'Ingénierie des Protéines, Institut de Chimie B6, Université de Liège, 4000 Liège, Belgium

<sup>b</sup>Department of Biochemistry and Molecular Biology, Jožef Stefan Institute, 1000 Ljubljana, Jamova 39, Slovenia

Received 11 April 2001; revisions requested 1 June 2001; revisions received 12 June 2001; accepted 19 June 2001

First published online 10 July 2001

## Abstract

**Background:** The stabilization of enzymes in the presence of substrates has been recognized for a long time. Quantitative information regarding this phenomenon is, however, rather scarce since the enzyme destroys the potential stabilizing agent during the course of the experiments. In this work, enzyme unfolding was followed by monitoring the progressive decrease of the rate of substrate utilization by the *Staphylococcus aureus* PC1  $\beta$ -lactamase, at temperatures above the melting point of the enzyme.

**Results:** Enzyme inactivation was directly followed by spectrophotometric measurements. In the presence of substrate concentrations above the  $K_m$  values, significant stabilization was observed with all tested compounds. A combination of unfolding kinetic measurements and enzymatic studies, both under steady-state and non-steady-state regimes, allowed most of the parameters characteristic of the two concurrent phenomena (i.e. substrate hydrolysis and enzyme denaturation) to be evaluated.

In addition, molecular modelling studies show a good correlation between the extent of stabilization, and the magnitude of the energies of interaction with the enzyme.

**Conclusions:** Our analysis indicates that the enzyme is substantially stabilized towards heat-induced denaturation, independently of the relative proportions of non-covalent Henri-Michaelis complex (ES) and acyl-enzyme adduct (ES\*). Thus, for those substrates with which the two catalytic intermediates are expected to be significantly populated, both species (ES and ES\*) appear to be similarly stabilized. This analysis contributes a new quantitative approach to the problem. © 2001 Elsevier Science Ltd. All rights reserved.

**Keywords:** Enzyme kinetics;  $\beta$ -Lactamase; Molecular modelling; Protein stability; Thermal unfolding

## 1. Introduction

The stability of many enzymes is dependent on the presence of substrates, co-factors or inhibitors. The strong and specific binding of the ligand to the native conformation generally results in a reduced sensitivity of the enzyme to heat-induced denaturation, possibly as a consequence of a conformational change or 'conformational tightening' [1–

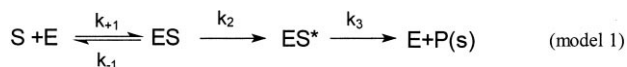
4]. With glucose oxidase [5], enhanced thermal stability results from the reduction of the enzyme during catalysis, but this change of electronic state is also probably associated with a subtle structural change of the enzyme. Binding of a metal ion was reported to increase the thermal stability of *Escherichia coli* RNase HI by up to  $\sim 12$  kJ/mol [6], due to the cancellation of charge repulsion around the active site. In a few cases [1,7,8], however, destabilization ('labilization') of the enzyme has also been reported. Although enzyme stabilization, and conversely destabilization, upon ligand binding have been well known for a long time (see also [9–11]), very few detailed quantitative analyses have been performed.

In order to understand this important phenomenon, we have investigated the thermal unfolding of two class A  $\beta$ -lactamases, produced by *Staphylococcus aureus* PC1 and *Streptomyces albus* G, in the presence of a variety

\* Corresponding author.

E-mail address: amatagne@ulg.ac.be (A. Matagne).

of substrates.  $\beta$ -Lactamases are bacterial enzymes which catalyze the irreversible hydrolysis of the amide bond of the  $\beta$ -lactam ring of penicillins and related antibiotics, yielding biologically inactive product(s) [12,13]. Most  $\beta$ -lactamases display an active site serine and, on the basis of their amino acid sequences, are divided into three molecular classes A, C and D. With most substrates, these enzymes function by a three-step mechanism:



where E is the enzyme, S the antibiotic, ES a non-covalent Henri-Michaelis complex,  $ES^*$  a covalent acyl-enzyme, and P(s) the inactive degradation product(s) of the antibiotic. According to this model, the steady-state parameters  $k_{\text{cat}}$  and  $K_m$  are related to the microscopic rate constants by the following equations:

$$k_{\text{cat}} = k_2 \times k_3 / (k_2 + k_3) \quad (1)$$

$$K_m = k_3 \times K' / (k_2 + k_3) \quad (2)$$

$$K' = (k_{-1} + k_2) / k_{+1} \quad (3)$$

Remarkably, with the *S. aureus* PC1  $\beta$ -lactamase, it was shown [14] that the values of the acylation ( $k_2$ ) and deacylation ( $k_3$ ) rate constants for benzylpenicillin and related penicillin substrates are approximately the same. Conversely, the acyl-enzyme intermediate accumulates during turnover of cephalosporins containing good leaving groups at the C-3' position [15], i.e. deacylation is the rate-limiting step ( $k_3 \ll k_2$ ).

The folding process of the *S. aureus* PC1  $\beta$ -lactamase has been studied in some details [16–19]. It constitutes a good model for protein folding studies, being one of the largest single domain proteins under investigation. It exhibits a thermodynamically stable partially folded state in the presence of 0.8 M guanidinium chloride (20°C, pH 7; [16]), and kinetic intermediates accumulate during the refolding reaction [16]. Stability measurements [20] revealed that heat-induced denaturation of the *S. aureus* PC1  $\beta$ -lactamase is fully reversible, whereas that of the *S. albus* G enzyme is not.

In this work, we have studied the thermal unfolding of the *S. aureus* PC1 and *S. albus* G  $\beta$ -lactamases. The presence of sufficiently high substrate concentrations ( $> K_m$ ) significantly stabilized both enzymes, but this phenomenon could only be quantitatively analyzed with the former, because denaturation of the latter was not fully reversible. Not surprisingly, the degree of stabilization depended upon the substrate structure, and appeared to be correlated with the enzyme–substrate energy of interaction. We present data obtained in the presence of various  $\beta$ -lactam compounds, using fluorescence and activity measurements. These data indicate that during turnover of the substrate, a substantial reduction in the rate of enzyme inactivation can occur.

## 2. Results and discussion

### 2.1. Thermal unfolding of class A $\beta$ -lactamases

The heat-induced equilibrium transition of the *S. aureus* PC1  $\beta$ -lactamase (Fig. 1) was determined by intrinsic fluorescence and catalytic activity measurements. Both methods indicate that the enzyme unfolds in a single transition ( $T_m \approx 41.5^\circ\text{C}$ ), which can be analyzed by assuming a two-state folding mechanism (Eq. 1). The good coincidence of the two curves in Fig. 1 suggests that both fluorescence and activity measurements monitor the same process, namely thermal unfolding and concomitant inactivation of the enzyme. Hence, with the *S. aureus* PC1 enzyme, inactivation and denaturation can be considered interchangeably.

By contrast, thermal inactivation of the *S. albus* G enzyme is irreversible and concentration-dependent. Thus, when enzyme concentrations of  $1.25 \text{ mg ml}^{-1}$  and  $1.25 \times 10^{-3} \text{ mg ml}^{-1}$  are incubated at  $45^\circ\text{C}$ , inactivation rate constant values of  $(0.4 \pm 0.05) \times 10^{-3} \text{ s}^{-1}$  ( $t_{1/2} \sim 30 \text{ min}$ ) and  $(0.2 \pm 0.03) \times 10^{-3} \text{ s}^{-1}$  ( $t_{1/2} \sim 60 \text{ min}$ ) are found, respectively. This phenomenon could be due to enzyme aggregation.

The unfolding kinetics of the *S. aureus* PC1  $\beta$ -lactamase, in the absence of substrate, were monitored by fluorescence spectroscopy at various temperatures, and analyzed according to a single exponential function, yielding the rate constant values listed in Table 1. At  $45^\circ\text{C}$ , the *S. aureus* PC1  $\beta$ -lactamase displays a lower half-life value

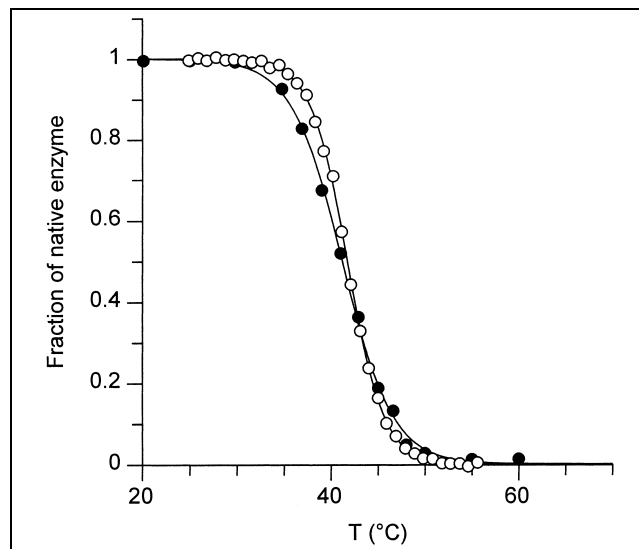


Fig. 1. Thermal unfolding transition of *S. aureus* PC1  $\beta$ -lactamase determined by measurements of intrinsic fluorescence ( $\circ$ ) and catalytic activity ( $\bullet$ ). Data have been normalized such that the value of the native state is 1. Both sets of data were analyzed on the basis of a two-state model and the lines represent the best fit to Eq. 1, calculated using  $T_m = 41.8 \pm 0.3^\circ\text{C}$  and  $41.2 \pm 0.6^\circ\text{C}$ , and  $\Delta H_m = 420 \pm 30 \text{ kJ mol}^{-1}$  and  $300 \pm 30 \text{ kJ mol}^{-1}$ , for fluorescence and activity measurements, respectively. The latter were performed with 1 mM benzylpenicillin, as described in Section 4.

Table 1

Effect of substrates on the unfolding rate constant ( $k_u$ ) of the *S. aureus* PC1  $\beta$ -lactamase measured in the temperature range from 40°C to 60°C

Ligand	$10^3 \times k_u$ (s <sup>-1</sup> )					$K_{m,30}$ ( $\mu$ M)	Energy of interaction (kJ/mol) <sup>b</sup>
	40°C	45°C	50°C	55°C	60°C		
None <sup>c</sup>	2.9	10.5	35	–	–	–	–
Cephalosporin C <sup>d</sup>	3.2	6.8	48	–	–	370	–
Cefazolin	–	< 1	10	41	–	1.4	178
6-Aminopenicillanic acid	< 1	1.6	9.6	30	–	170	162
Penicillanic acid	< 1	4	10.5	22	–	200	147
Ampicillin	–	–	< 1	2.9	8.3	15	239
Nitrocefin	–	–	< 1	2.6	15.4	1.5	265
Cephaloglycin	–	–	< 1	2	> 70	3	231
Benzylpenicillin	–	–	< 1	1.8	> 70	3	212

Fluorescence and activity measurements were performed as described in Section 4. With all substrates (except cephalosporin C, see text), experiments were performed at saturating concentrations ( $[S]/K_{m,30} \approx 50^\circ$ ). The standard deviation for  $k_u$  is about 10%. (–) Not determined.

<sup>a</sup>Values obtained at 30°C (A. Matagne, A. Lejeune and J.M. Frère, unpublished data). Measurements performed between 40°C and 60°C with some substrates indicated that the  $K_m$  is increased by a factor of 10, or less at the highest temperature. It is assumed to be similar for all compounds, and hence the substrate concentration can be considered as close to saturation ( $[S]/K_m \geq 5$ ) at all temperatures.

<sup>b</sup>Calculated total energy of interaction (absolute values) during formation of the Henri-Michaelis complexes between the *S. aureus* PC1  $\beta$ -lactamase and the various substrates. Note that similar values were obtained [37] for the Henri-Michaelis complexes formed between the *S. albus* G  $\beta$ -lactamase and benzylpenicillin (151 kJ/mol) and cephalosporin C (197 kJ/mol).

<sup>c</sup>Fluorescence measurements.

<sup>d</sup>Activity measurements performed with 50  $\mu$ M ( $< 0.1 \times K_m$ ) cephalosporin C.

( $t_{1/2} \sim 1$  min) than the *S. albus* G enzyme ( $t_{1/2} \geq 30$  min), which correlates with its lower thermodynamic stability [20].

A typical thermal unfolding trace, monitored continuously during substrate turnover, is shown in Fig. 2. In these experiments, less than 25% of the substrate is utilized and the kinetics can be fitted to Eq. 6, with the appropriate correction when  $[S] < K_m$ , thus yielding the various rate constant values ( $k_u$ ) for thermal inactivation of the *S. aureus* PC1 enzyme, in Table 1. When the substrate concentration can be chosen far below the  $K_m$  value (cephalosporin C,  $[S]/K_m < 0.1$ , see Table 1), the rate constant of enzyme unfolding display values similar to those determined by intrinsic fluorescence measurements, i.e. in the absence of substrate (Table 1). At saturating substrate concentrations ( $[S]/K_m \geq 5$ , see Table 1), however, a sig-

nificant reduction in the rate of enzyme inactivation is observed. A markedly higher degree of stabilization of the enzyme is achieved by increasing the concentration of the substrate present during the inactivation reaction. This is illustrated in Fig. 3, where thermal inactivation of the enzyme is monitored at 52°C in the presence of cefazolin as reporter substrate ( $K_m \approx 13$   $\mu$ M, see below), in a concentration range from 20 to 350  $\mu$ M. Maximum protection of the enzyme is observed when  $[S]/K_m \geq 8$ . A similar effect was observed when using 6-aminopenicillanic acid (2–18 mM, with maximum protection  $\sim 10$  mM) and nitrocefin (60–360  $\mu$ M, with maximum protection  $\sim 200$   $\mu$ M) as substrates. Nevertheless, due to its relatively low  $k_{cat}$  and  $K_m$  values (2.1 s<sup>-1</sup> and 13  $\mu$ M, respectively, at 52°C), cefazolin is the best substrate for further investigations of the thermal unfolding behavior of the *S. aureus*

Table 2

Effect of substrates on the unfolding rate constant ( $k_u$ ) of the *S. albus* G  $\beta$ -lactamase at 56°C

Substrate	Concentration ( $\mu$ M)	$K_{m,30}$ ( $\mu$ M) <sup>a</sup>	$10^3 \times k_u$ (s <sup>-1</sup> )
Benzylpenicillin	1 000	1 000	21 $\pm$ 3
	2 000		12 $\pm$ 1.5
Ampicillin	1 000	650	18.6 $\pm$ 1
	2 000		16 $\pm$ 1.5
6-Aminopenicillanic acid	1 000	200	12 $\pm$ 1
	2 000		16 $\pm$ 1.5
Carbenicillin	1 000	> 10 000	38 $\pm$ 7
	4 000		24 $\pm$ 2
Cephaloridine	100	320	31 $\pm$ 2
	200		25 $\pm$ 2
Cephalosporin C	200	4 500	30.5 $\pm$ 2
	400		32 $\pm$ 2

Values were obtained by activity measurements, in the presence of various substrates, as described in Section 4.

<sup>a</sup>Values at 30°C [14]. Measurements with both benzylpenicillin and ampicillin on the temperature range from 20°C to 50°C (A. Matagne and J.M. Frère, unpublished data) indicated that the  $K_m$  values decrease slightly ( $K_{m,20}/K_{m,50} = 2$ –3) at higher temperatures.

PC1  $\beta$ -lactamase during turnover, since it allows complete unfolding time-courses to be monitored at substrate saturation, without significant substrate depletion and in a reasonably high enzyme concentration range.

Measurements of the initial ( $v_0$ ) and steady-state ( $v_{ss}$ ) rate values for the kinetic experiment at 52°C in Fig. 2 indicate that  $\sim 4\%$  ( $v_{ss}/v_0 = 0.04$ ) of the enzyme remains active. This result contrasts with the thermal unfolding curves in Fig. 1, which indicate that virtually complete denaturation/inactivation of the enzyme occurs at 52°C. This apparent discrepancy can easily be explained by the enhanced stability of the enzyme during substrate turnover. In principle, by measuring  $v_0$  and  $v_{ss}$  at various temperatures, it should be possible to obtain the thermal unfolding curve of the enzyme in the presence of substrate. This proved, however, to be technically difficult, especially at  $T \leq T_m$  where enzyme inactivation occurs very slowly ( $t_{1/2} > 1\text{h}$ ). Under these conditions, the reporter substrate method is not practical. Nevertheless, the data (not shown) obtained at  $T \geq T_m$  bring further evidence in favor of the enhanced thermodynamic stability of the enzyme in the presence of substrate, consistently with its reduced  $k_u$  values.

Similar experiments performed with the *S. albus* G  $\beta$ -lactamase (Table 2) indicate that this enzyme is also

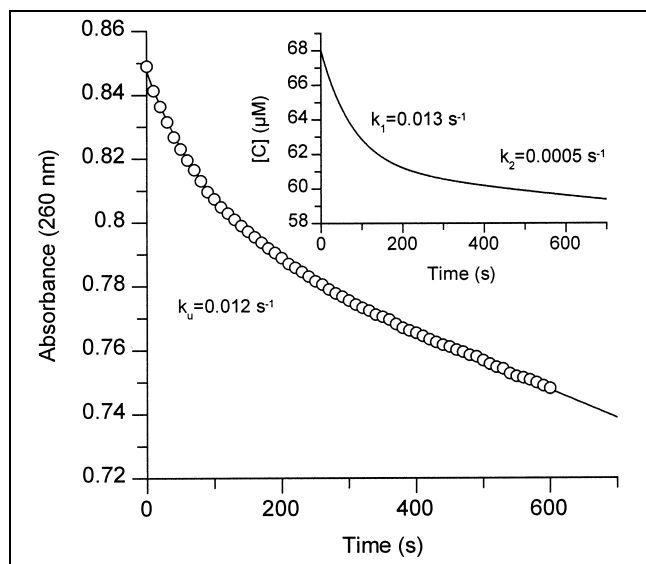


Fig. 2. The rate of thermal inactivation of *S. aureus* PC1  $\beta$ -lactamase in the presence of cefazolin. The enzyme ( $0.05 \mu\text{M}$ ) was incubated at 52°C with  $68 \mu\text{M}$  cefazolin in 50 mM sodium phosphate buffer, pH 7. Hydrolysis of the reporter substrate was monitored by recording the decrease in absorbance at 260 nm and, according to the method described in [46], an apparent first-order rate constant ( $k_u$ ) value of  $0.012 \pm 0.001 \text{ s}^{-1}$  was computed. The curve represents the best fit of the data to Eq. 6, modified as in [46]. Note that spontaneous hydrolysis of cefazolin occurs throughout the time-course of the experiment. However, this phenomenon does not account for more than 8% of substrate utilization and can thus be considered as occurring at a constant rate. It only influences the  $v_0$  and  $v_{ss}$  values, and not  $k_u$ . After correction for this phenomenon,  $v_0 = 5.73 \mu\text{mol min}^{-1} \text{ mg}^{-1}$  and  $v_{ss} = 0.24 \mu\text{mol min}^{-1} \text{ mg}^{-1}$ . The inset shows the simulated kinetics (see text).

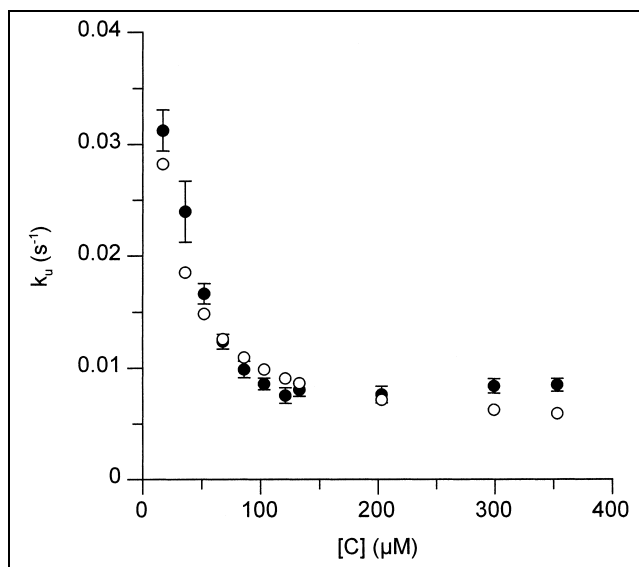


Fig. 3. Influence of the concentration of cefazolin on the inactivation rate ( $k_u$ ) of the *S. aureus* PC1  $\beta$ -lactamase at 52°C. ● Experimental data. These values were obtained as described in Section 4 (see also Fig. 2). ○ Simulated data computed on the basis of model 2, as described in the text. Values given in Table 3 were used for  $k_{cat}$ ,  $K_m$ ,  $k_2$ ,  $k_3$ ,  $K'$ ,  $k_{u,1}$  and  $k_{f,1}$ , with  $k_{u,2} = 3 \times 10^{-3} \text{ s}^{-1}$ ,  $k_{f,2} = 0.039 \text{ M}^{-1} \text{ s}^{-1}$ ,  $k_{u,3} = 3 \times 10^{-3} \text{ s}^{-1}$  and  $k_{f,3} = 1.5 \times 10^{-3} \text{ s}^{-1}$ .

significantly stabilized in the presence of substrate at concentrations  $\geq K_m$ . The *S. aureus* PC1 enzyme is, however, a more favorable subject for further investigation of this phenomenon. Thermal inactivation of this enzyme is fully reversible, and occurs at relatively low temperature ( $T_m = 41.5^\circ\text{C}$ ) in comparison with the *S. albus* G enzyme and other class A  $\beta$ -lactamases [20]. This is critical in order to monitor enzyme inactivation by the reporter substrate method, in a temperature range where  $\beta$ -lactam compounds are sufficiently stable on the time scale of the experiment. This would be technically much more difficult with, for instance, the TEM-1 ( $T_m = 50^\circ\text{C}$  [20]) or the *Bacillus licheniformis* ( $T_m = 63^\circ\text{C}$  [20]) enzymes. In addition, all the kinetic constants in model 1 can be determined with the *S. aureus* PC1  $\beta$ -lactamase and cefazolin (see below).

Model 2 (Section 4) has been used to describe the thermal stabilization of the *S. aureus* PC1  $\beta$ -lactamase in the presence of substrate. To test this model, we compared the experimental and calculated values of the inactivation rate constant ( $k_u$ ) of the enzyme at 52°C, in the presence of cefazolin concentrations ranging from 17 to 350  $\mu\text{M}$  (Fig. 3). This analysis indicates that model 2 is suitable for the description of the data.

## 2.2. Evaluation of the kinetic constants in model 2

In this section we describe how the 11 kinetic constants (i.e.  $k_{u,1}$ ,  $k_{f,1}$ ,  $k_{u,2}$ ,  $k_{f,2}$ ,  $k_{u,3}$ ,  $k_{f,3}$ ,  $k_2$ ,  $k_3$ ,  $k_{cat}$ ,  $K'$  and  $K_m$ ), which define parameters  $A$ ,  $B$ ,  $D$ ,  $F$  and  $G$  (Eqs. 13–17)

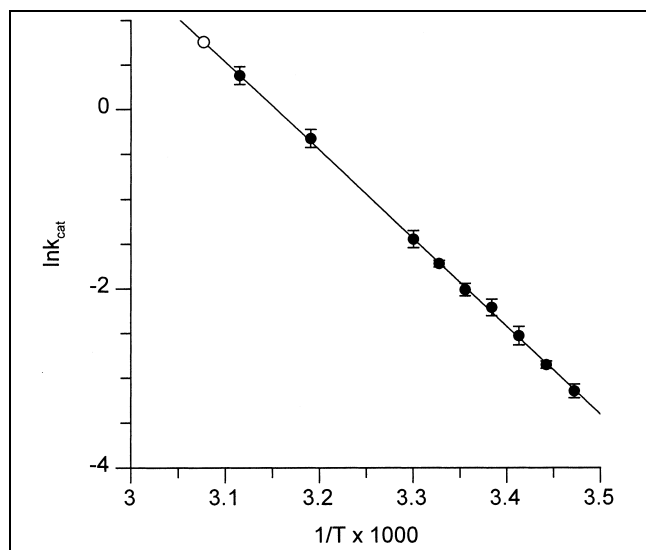


Fig. 4. Temperature dependence of the turnover number ( $k_{\text{cat}}$ ) for *S. aureus* PC1  $\beta$ -lactamase and cefazolin, shown as an Arrhenius plot.  $k_{\text{cat}}$  has units of  $\text{s}^{-1}$  and  $T$  has units of K. (●) Measured values; (○) extrapolated value at 52°C ( $k_{\text{cat}} = 2.1 \text{ s}^{-1}$ ). Errors are given as standard deviations. The continuous line is the best fit to  $\ln k_{\text{cat}} = \ln A - E_a/RT$ , with  $E_a = 82 \pm 2 \text{ kJ mol}^{-1}$ .

can be derived. Direct measurements at 52°C are not possible, and thus some extrapolations are needed.

The steady-state parameters  $k_{\text{cat}}$  and  $K_m$  were determined between 17°C and 48°C. Above this temperature, significant enzyme inactivation occurs on the time scale of the kinetic experiment, and no data could be obtained. Up to 48°C, however, a typical Arrhenius temperature dependence of the turnover number ( $k_{\text{cat}}$ ) is observed (Fig. 4), which allows the  $k_{\text{cat}}$  value ( $2.1 \text{ s}^{-1}$ ) at 52°C to be obtained by extrapolation with a good confidence. Interestingly, the simple Arrhenius behavior of  $k_{\text{cat}}$  (Eq. 1) suggests that  $k_2$  and  $k_3$  display the same temperature dependence, or alternatively, that one of the two catalytic steps (i.e. acylation or deacylation) in model 1 is consistently rate-limiting (i.e.  $k_{\text{cat}} = k_2$  or  $k_{\text{cat}} = k_3$ , see below).  $K_m$  is a function of the four microscopic rate constants in model 1 (i.e.  $k_{+1}$ ,  $k_{-1}$ ,  $k_2$ , and  $k_3$ , see Eq. 2), and thus a complex temperature dependence of this parameter could be expected. Nevertheless, a linear relationship appears to prevail between  $\ln K_m$  and  $T$  (Fig. 5), leading to an approximate value of 13  $\mu\text{M}$  at 52°C.

The rate constant values for acylation ( $k_2$ ) and deacylation ( $k_3$ ) could be measured under non-steady-state conditions, using stopped-flow measurements. These experiments were performed between 15°C and 30°C, at intervals of 2.5°C. Under these conditions, the population of unfolded enzyme species is negligible (Fig. 1). In all cases, the stoichiometry of the burst (see Eq. 7) was found to be close to unity ( $B \sim 1$ ), suggesting that the interaction between cefazolin and the *S. aureus* PC1  $\beta$ -lactamase can be interpreted on the basis of model 1, with  $k_3 \ll k_2$  (i.e.  $k_{\text{cat}} = k_3$ ). Thus, no branched pathway [15] needs to be

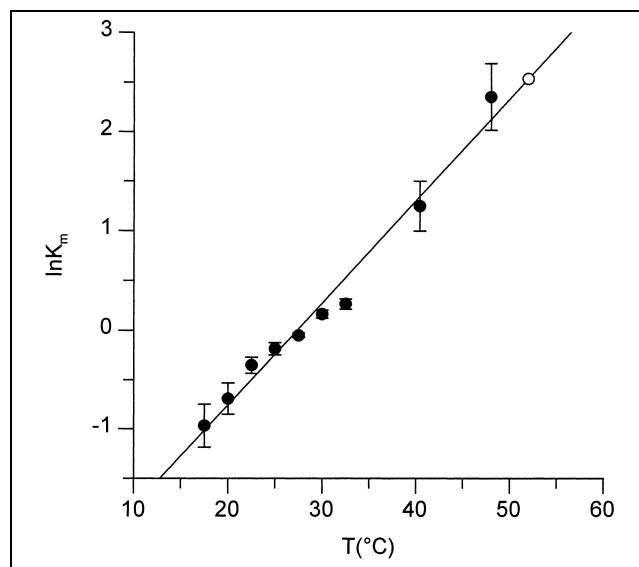


Fig. 5. Temperature dependence of  $K_m$  for *S. aureus* PC1  $\beta$ -lactamase and cefazolin.  $K_m$  has units of  $\mu\text{M}$ . (●) Measured values; (○) value at 52°C ( $K_m \approx 13 \mu\text{M}$ ) based on linear extrapolation. Errors are given as standard deviations.

considered, although the presence of a good leaving group on C-3' of cefazolin suggests that the acyl-enzyme is probably the rearranged adduct.

The dependence of the rate constant for acyl-enzyme formation ( $k_a$ ) on cefazolin concentration at 22.5°C is shown in Fig. 6. Similar experiments were performed at each temperature, and fitting the various data to Eq. 8 provides values of  $k_2$ ,  $k_3$  and  $K'$  in the temperature range from 15°C to 30°C (data not shown). The values of  $k_3$  are in reasonable agreement with those of  $k_{\text{cat}}$  determined at

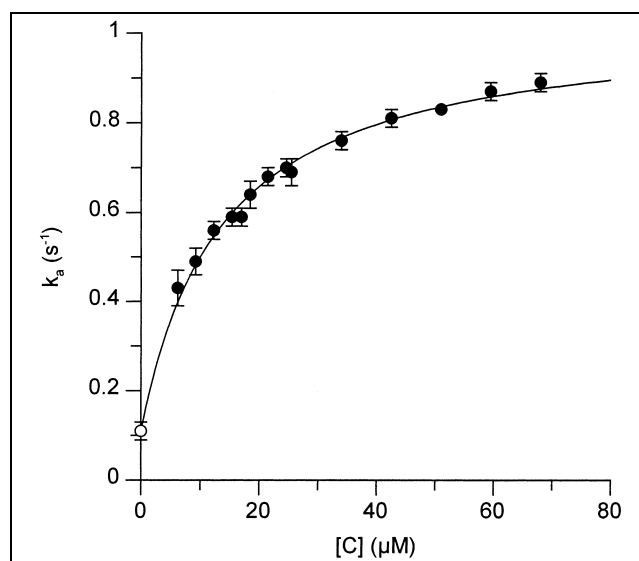


Fig. 6. Kinetics of interaction between *S. aureus*  $\beta$ -lactamase and cefazolin at 22.5°C. Variation of  $k_a (= k_3 + (k_2 \times [S]) / (K' + [S]))$  with cefazolin concentration. (●) Stopped-flow measured values; (○)  $k_{\text{cat}}$  (see text). The data were fitted (full line) to Eq. 8, yielding  $k_2 = 0.92 \pm 0.02 \text{ s}^{-1}$  and  $K' = 13.5 \pm 0.8 \mu\text{M}$ .

the steady-state. In the pre-steady-state experiments, however, concentrations of cefazolin below 10  $\mu\text{M}$  (i.e. below the  $K'$  value) give very small absorbance variations ( $\Delta A < 0.08$ ), and hence yield very inaccurate data. In consequence, it appears that fitting of the data to Eq. 8 gives better results when the value of  $k_a$  at  $[C] = 0$  (i.e.  $k_a = k_3$ ) is taken as the  $k_{\text{cat}}$  value, and is considered as an additional experimental point in the analysis. This is especially critical at the lowest temperatures where the  $K'$  value is low ( $K' = 13.5 \mu\text{M}$  at  $22.5^\circ\text{C}$ ). The temperature dependence of  $k_2$  is shown in Fig. 7. The Arrhenius-like behavior of the temperature dependence of the acylation rate constant ( $k_2$ ) indicates a value of  $45 \text{ s}^{-1}$  at  $52^\circ\text{C}$ . Assuming a linear temperature dependence of  $\ln K'$  (not shown) leads to an approximate value of  $68 \mu\text{M}$  at  $52^\circ\text{C}$ . The extrapolated values of  $k_2$  ( $45 \text{ s}^{-1}$ , Fig. 7) and  $k_3$  ( $= k_{\text{cat}} = 2.1 \text{ s}^{-1}$ , Fig. 4) at  $52^\circ\text{C}$ , and the estimated value of  $K_m$  ( $\sim 13 \mu\text{M}$ , Fig. 5) allow computation of  $K' (= k_2/k_3 \times K_m) = 280 \mu\text{M}$ . Conversely, a  $K'$  value of  $68 \mu\text{M}$  leads to  $K_m = 3.2 \mu\text{M}$ . The fact that these two values for  $K'$  and  $K_m$  are not very different suggests that they are reasonable estimates at  $52^\circ\text{C}$ . In our simulations (see below), we use  $K' = k_2/k_{\text{cat}} \times K_m (= 280 \mu\text{M})$ .

The values of the microscopic rate constants for unfolding ( $k_{u,1}$ ) and refolding ( $k_{f,1}$ ) of the free protein ( $E+E'$ ) could be estimated from the intrinsic fluorescence experiments, performed at equilibrium and far from the transition zone.

In the transition range ( $35^\circ\text{C}$  to  $50^\circ\text{C}$ ) of the thermal denaturation curve (Fig. 1), the values of  $K_{u,1} (= k_{u,1}/k_{f,1})$  can be analyzed according to the van't Hoff equation ([21]; Fig. 8a). Similarly, the temperature dependence (be-

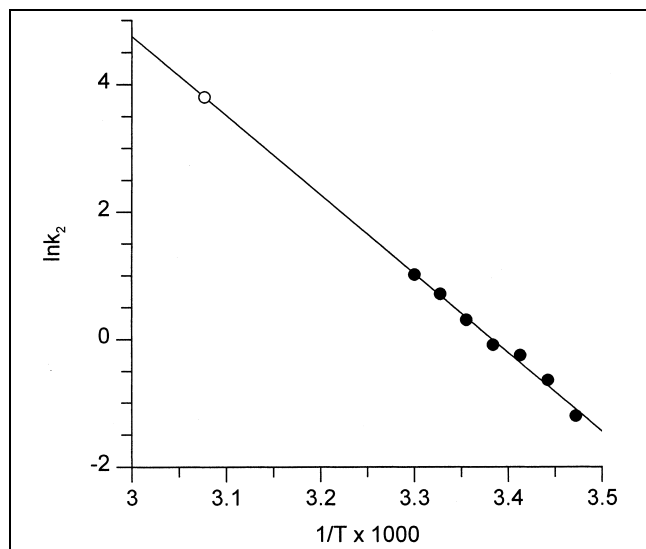


Fig. 7. Temperature dependence of the acylation rate constant ( $k_2$ ) for *S. aureus* PC1  $\beta$ -lactamase and cefazolin, shown as an Arrhenius plot.  $k_2$  has units of  $\text{s}^{-1}$  and  $T$  has units of K. (●) Measured values; (○) extrapolated value at  $52^\circ\text{C}$  ( $k_2 = 45 \text{ s}^{-1}$ ). Errors (S.D. values) on these measurements are  $< 10\%$ . The continuous line is the best fit to  $\ln k_2 = \ln A - E_a/RT$ , with  $E_a = 103 \pm 5 \text{ kJ mol}^{-1}$ .

tween  $40^\circ\text{C}$  and  $60^\circ\text{C}$ ) of the unfolding rate constant ( $k_u = k_{u,1} + k_{f,1}$ ) values can be analyzed according to the Arrhenius equation (Fig. 8b). By combining these data, the values of  $k_{u,1}$  (Fig. 8c) and  $k_{f,1}$  (Fig. 8d) can be computed between  $40^\circ\text{C}$  and  $50^\circ\text{C}$ . Above  $50^\circ\text{C}$ ,  $k_{u,1} = k_u$  ( $k_{u,1} \gg k_{f,1}$ ) and thus can be determined experimentally ( $k_{u,1} = 6 \times 10^{-2} \text{ s}^{-1}$ , at  $52^\circ\text{C}$ ). Fig. 8d shows that there is a marked curvature in the Arrhenius plot for the temperature dependence of  $k_{f,1}$ . Non-Arrhenius kinetics is a common phenomenon for protein refolding reactions, and is due, at least in part, to a relatively large change in heat capacity ( $\Delta C_p^\#$ ) between the unfolded and the transition state for the folding transition [22–26]. Following the analysis of Chen et al. [22], the temperature dependence of the microscopic rate constant  $k_{f,1}$  can be analyzed according to Eq. 4:

$$k_i = \exp[A_i + B_i (T^\circ/T) + C_i \ln (T^\circ/T) + \ln T] \quad (4)$$

where:

$$A_i = [-\Delta C_{\text{pi}}^\# + \Delta S_i^\# (T^\circ)]/R + \ln (k_B/h)$$

$$B_i = [\Delta C_{\text{pi}}^\# - \Delta S_i^\# (T^\circ)]/R - \Delta C_i^\# (T^\circ)/RT^\circ$$

$$C_i = -\Delta C_{\text{pi}}^\#/R$$

and  $T^\circ$  is the reference temperature ( $293.15 \text{ K}$  in our calculations),  $k_B$ ,  $h$  and  $R$  are the Boltzmann, Planck, and gas constants, respectively.  $\Delta G_i^\#$ ,  $\Delta S_i^\#$  and  $\Delta C_{\text{pi}}^\#$  are the free energy of activation, the entropy of activation, and the heat capacity change between the denatured and the transition states, respectively.

As shown in Fig. 8d, the temperature dependence of the microscopic refolding rate constant ( $k_{f,1}$ ) is adequately described by the above equation, yielding  $\Delta G_{\text{UN}}^\# = 95.4 \text{ kJ mol}^{-1}$ ,  $\Delta S_{\text{UN}}^\# = 2.1 \text{ kJ mol}^{-1} \text{ K}^{-1}$  and  $\Delta C_{\text{pUN}}^\# = -33.3 \text{ kJ mol}^{-1} \text{ K}^{-1}$ . Extrapolation to  $52^\circ\text{C}$  gives a value of  $k_{f,1} = 2.2 \times 10^{-4} \text{ s}^{-1}$ .

Unlike protein refolding reactions, there is relatively little change in exposure of hydrophobic residues between the native state and the transition state on unfolding and, hence, the activation heat capacity for unfolding is small. The transition state ensemble for the folding process of a variety of proteins is somewhat expanded and loosely packed compared to the native state, although still globally collapsed and excluding water, thus roughly resembling the folded state [27–33]. Consistent with these findings, Fig. 8c shows no significant deviation from standard Arrhenius-type behavior. A similar observation was made with hen lysozyme [34] chymotrypsin inhibitor 2 [35], protein G [36], CspB [24] and protein L [25].

The curves in Fig. 8c,d intersect to a  $T_m$  value of  $41.4^\circ\text{C}$ , in agreement with the values ( $41.8^\circ\text{C}$  and  $41.2^\circ\text{C}$ ) obtained in equilibrium folding experiments (Fig. 1).

The values of the four microscopic rate constants ( $k_{u,2}$ ,

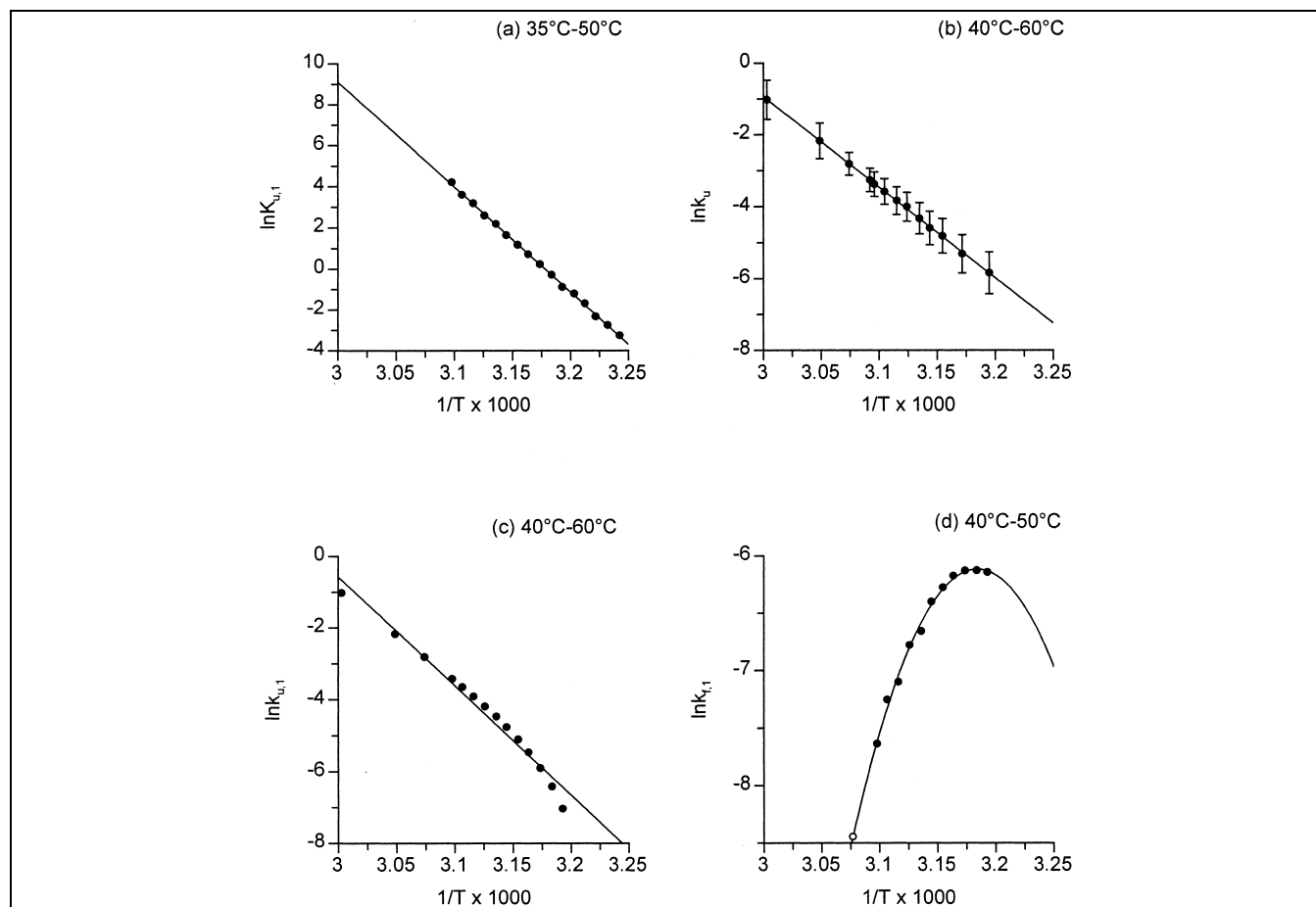


Fig. 8. Temperature dependence of the equilibrium constant ( $K_{u,1}$ ) and of the microscopic rate constants for unfolding ( $k_{u,1}$ ) and refolding ( $k_{f,1}$ ) of the free *S. aureus* PC1  $\beta$ -lactamase.  $K_{u,1}$  has no units,  $k_u$ ,  $k_{u,1}$  and  $k_{f,1}$  have units of  $s^{-1}$ , and  $T$  has units of K. (a) van't Hoff plot of  $K_{u,1} = k_{u,1}/k_{f,1}$ . The continuous line is the best fit to  $\ln K = -\Delta H/RT + \Delta S/R$ , with  $\Delta H = 425 \pm 10$  kJ mol<sup>-1</sup> and  $\Delta S = 1.35 \pm 0.02$  kJ mol<sup>-1</sup> K<sup>-1</sup>. (b) Arrhenius plot of  $k_u = k_{u,1} + k_{f,1}$ . The continuous line is the best fit to  $\ln k_u = \ln A - E_a/RT$ , with  $E_a = 210 \pm 3$  kJ mol<sup>-1</sup>. (c) Arrhenius plot of  $k_{u,1}$ . The continuous line is the best fit to  $\ln k_{u,1} = \ln A - E_a/RT$ , with  $E_a = 250 \pm 10$  kJ mol<sup>-1</sup>. Note that values at 52°C, 55°C and 60°C were determined experimentally ( $k_{u,1} = k_u$ ). (d) Arrhenius plot of  $k_{f,1}$ . The continuous line is the best fit to Eq. 4. The activation parameters derived from this fit are  $\Delta G_{UN}^\ddagger = 95.4$  kJ mol<sup>-1</sup>,  $\Delta S_i^\ddagger = 2.1$  kJ mol<sup>-1</sup> K<sup>-1</sup> and  $\Delta C_{pi}^\ddagger = -33.3$  kJ mol<sup>-1</sup> K<sup>-1</sup>. The extrapolated  $k_{f,1}$  ( $2.2 \times 10^{-4}$  s<sup>-1</sup>) value at 52°C is represented by an open circle.

$k_{f,2}$ ,  $k_{u,3}$ ,  $k_{f,3}$ ), corresponding to the unfolding equilibrium of the non-covalent (ES) and covalent (ES\*) enzyme-substrate complexes, are not accessible and were chosen arbitrarily. Thus, both  $k_{u,2}$  and  $k_{u,3}$  were taken as  $k_{u,1}/20$  ( $= 3 \times 10^{-3}$  s<sup>-1</sup>) to take into account the stabilization of the kinetic intermediate species. The value of  $k_{f,2}$  ( $= 0.039$  M<sup>-1</sup> s<sup>-1</sup>) is determined by the equilibrium relationship between E, E' and ES, i.e.  $K_{u,2} = K_{u,1} \times K'$ . Fixing  $K_{u,3} = 2$  leads to  $k_{f,3} = 1.5 \times 10^{-3}$  s<sup>-1</sup>.

The values of the various constants that define parameters  $A$ ,  $B$ ,  $D$ ,  $F$  and  $G$  are given in Table 3.

### 2.3. Analysis of the unfolding kinetics

As indicated in Section 4, we have used model 2 to describe the influence of cefazolin on the thermal stability of the *S. aureus* PC1  $\beta$ -lactamase at 52°C. The experimental data were simulated using Eqs. 9–17. On the basis of the values estimated for the various constants (Table 3) which define the parameters  $A$ ,  $B$ ,  $D$ ,  $F$  and  $G$ , the

time-courses of the concentrations of the native ( $x$ , Eq. 9) and unfolded ( $y$  and  $z$ , Eqs. 10 and 11) enzyme species could be simulated (Fig. 9) at substrate concentrations ranging from 17 to 350  $\mu$ M. Similarly, by using Eq. 12

Table 3  
Values at 52°C of the kinetic constants used in model 2

Parameters	Values
$k_{cat}$	2.1 s <sup>-1</sup>
$K_m$	13 $\mu$ M
$k_3 = k_{cat}$	2.1 s <sup>-1</sup>
$k_2$	45 s <sup>-1</sup>
$K' = (k_2/k_{cat}) \times K_m$	280 $\mu$ M
$k_{u,1}$	$6 \times 10^{-2}$ s <sup>-1</sup>
$k_{f,1}$	$2.2 \times 10^{-4}$ s <sup>-1</sup>
$k_{u,2}^a$	$(0.10-6) \times 10^{-2}$ s <sup>-1</sup>
$k_{f,2} = k_{u,2}/(K_{u,1} \times K')$	$0.015-1$ M <sup>-1</sup> s <sup>-1</sup>
$k_{u,3}^a$	$(0.01-1) \times 10^{-2}$ s <sup>-1</sup>
$k_{f,3}^a$	$(0.001-0.75) \times 10^{-2}$ s <sup>-1</sup>

<sup>a</sup>The values of these parameters had to be fixed arbitrarily. In each case, a range of values is given which fit the experimental data (see text).

the kinetics of substrate hydrolysis could also be computed (Fig. 2).

At all substrate concentrations, the time-courses of  $x$ ,  $y$  and  $z$  correspond to the sums of two exponential functions. The kinetics of  $E'$  and  $E'S^*$  formation (Fig. 9), i.e. enzyme denaturation, indicate that most of the enzyme is inactivated under its free form ( $E \rightarrow E'$ ), and not as an acyl-enzyme ( $ES^* \rightarrow E'S^*$ ). The kinetics (Fig. 9) of depletion of the native ( $E+ES+ES^*$ ) enzyme species are in a good agreement with the thermal inactivation curves (Fig. 2) observed in the presence of the reporter substrate. Indeed, at all substrate concentrations the value of the rate constant for the first major phase (e.g. 97% amplitude and  $k_1 = 13 \times 10^{-3} \text{ s}^{-1}$  at 68  $\mu\text{M}$  cefazolin) obtained in the simulations is consistent with the value measured in the inactivation experiments ( $k_u = 12 \times 10^{-3} \text{ s}^{-1}$  at 68  $\mu\text{M}$  cefazolin). The second minor phase (2% amplitude and  $k_2 = 5 \times 10^{-4} \text{ s}^{-1}$  at 68  $\mu\text{M}$  cefazolin) in the simulations, however, is not observed in the kinetic experiments. This is most likely due to both its very small amplitude and its low rate constant value ( $t_{1/2} \approx 20 \text{ min}$ ). Close examination of the kinetics of substrate hydrolysis (Fig. 2) indicates that the  $v_{ss}/v_0$  ratios measured at all concentrations correlate well with the corresponding calculated values (Fig. 10). All these observations bring compelling evidence that model 2 provides a good description of the inactivation phenomenon observed in the presence of substrate.

A series of alternative values was also tested for the parameters for which only rough estimates could be obtained (i.e.  $K_m$ ,  $k_{u,2}$  and  $k_{u,3}$ , and hence  $K'$ ,  $k_{f,2}$  and  $k_{f,3}$ , see above). Changing the value of  $K_m$  (and hence  $K'$  and  $k_{f,2}$ ) in a concentration range from 10 to 20  $\mu\text{M}$  resulted in no significant deviation between the simulated and calcu-

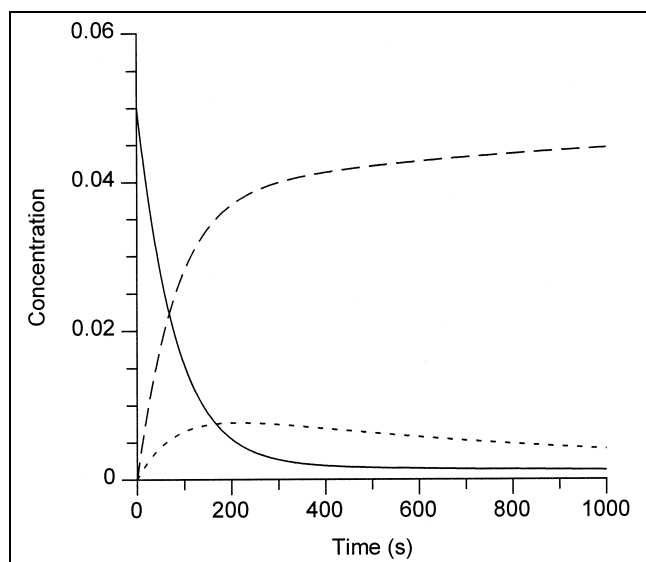


Fig. 9. Simulated time-courses at 52°C of the native and unfolded enzyme species in the presence of 68  $\mu\text{M}$  cefazolin. Model 2 and Eqs. 9–17 were used, with the parameter values given in Table 3 and in the legend of Fig. 3. The continuous line corresponds to  $x$  ( $=E+ES+ES^*$ ), the dashed line to  $y$  ( $=E'$ ) and the dotted line to  $z$  ( $=E'S^*$ ).

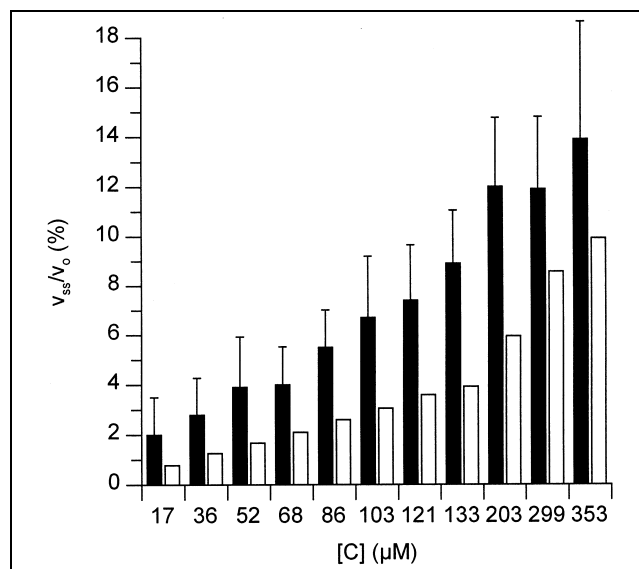


Fig. 10. Measured (filled bars) and calculated (empty bars)  $v_{ss}/v_0$  ratios as a function of cefazolin concentration.  $v_{ss}/v_0$  ratios were calculated on the basis of model 2, with the parameter values given in Table 3 and in the legend of Fig. 3.

lated  $k_u$  values, indicating that the relative uncertainty on the  $K_m$  value at 52°C has a negligible influence on the simulation. In contrast to  $K_m$ ,  $k_{u,2}$  and  $k_{u,3}$  could not be measured at any temperature, and thus had to be arbitrarily fixed. Simulations were performed with very different values for these parameters, i.e.  $k_{u,2} = (0.1\text{--}60) \times 10^{-2} \text{ s}^{-1}$  and  $k_{u,3} = (0.01\text{--}6) \times 10^{-2} \text{ s}^{-1}$ . In addition,  $K_{u,3}$  was allowed to vary between 0.4 and 10. No major deviation from the experimental data is observed when  $k_{u,2} < k_{u,1}$  and  $k_{u,3} < k_{u,1}/10$ . When  $0.1 < k_{u,3}/k_{u,1} < 1$ , the simulations indicate that the enzyme remains protected, but to a lesser extent than observed experimentally. By contrast, there is a strong discrepancy between the simulated and calculated  $k_u$  values when  $k_{u,2}$  or  $k_{u,3}$  are  $\geq k_{u,1}$ .

These important findings clearly demonstrate that when the substrate is bound, covalently ( $ES^*$ ) or not ( $ES$ ), the enzyme is significantly stabilized towards heat-induced denaturation. This is consistent with our observation that, with both the *S. albus* G and the *S. aureus* PC1  $\beta$ -lactamases, no protection is obtained at substrate concentrations far below the  $K_m$ , whereas maximum protection is achieved at saturating concentrations.

For a three-state model (model 1) where two distinct intermediate species occur, enzyme stabilization may be associated with the enhanced thermal stability of both the non-covalent complex ( $ES$ ) and the covalent adduct ( $ES^*$ ). With the *S. aureus* PC1  $\beta$ -lactamase and both cefazolin and cephaloglycin, the presence of a good C-3' leaving group leads to acyl-enzyme accumulation [15]. Thus, the acyl-enzyme is the only significantly populated species during hydrolysis of these substrates, i.e.  $[ES]$  is negligible, and hence the intrinsic value of  $k_{u,2}$  is irrelevant (with  $k_{u,2} < k_{u,1}$ ). This contrasts, however, with the hydro-



lysis of benzylpenicillin, for which Waley and co-workers [14] showed that the rate constant values for acylation and deacylation are approximately the same ( $k_{+2}/k_{+3} = 1.8$  at 20°C, pH 7). Consequently, in the presence of this substrate, the stability of the *S. aureus* PC1 enzyme is controlled by the stability of both ES and ES\*.

Interestingly, the data in Table 1 show that the extent of enzyme stabilization achieved with the different substrates can vary significantly ( $t_{1/2} = 20\text{--}400$  s at 55°C). Thus, data obtained at 55°C clearly indicate that benzylpenicillin and cephaloglycin are the most efficient substrates, whereas 6-aminopenicillanate and cefazolin are the poorest. This effect might, in principle, arise from a difference in stability between the non-covalent (ES) and the covalent (ES\*) adducts, which are populated to various extents at the steady-state, depending on the substrate. This possibility must, however, be discarded, since very similar  $k_u$  values are obtained with benzylpenicillin and cephaloglycin, although they display very different [ES]/[ES\*] ratios. On the contrary, with both cephaloglycin and cephalothin, the acyl-enzyme is by far the most populated species at the steady-state (>99% at saturating concentrations), but nevertheless the two compounds have markedly different effects on the stability of the enzyme. In consequence, the difference in stability observed with the various substrates tested is due, not to their different  $k_2/k_3$  ratios but, more probably, to their intrinsic binding properties.

#### 2.4. Modelling the interactions with *S. aureus* PC1 $\beta$ -lactamase

The  $\beta$ -lactam molecules used in this study (Table 1) were docked into the *S. aureus* PC1 active site. As previously described [37,38], the  $\beta$ -lactam carbonyl oxygen atom was located in the oxyanion hole formed by the backbone nitrogen atoms of Ser-70 and Gln-237, and the carboxylate group (on C-3 or C-4 of penicillin and cephalosporin substrates, respectively) was oriented towards the side-chain amino group of Lys-234. With all compounds, the energies of the corresponding non-covalent complexes were minimized as described in Section 4, allowing the total energy of interaction of the Henri-Michaelis complexes formed between the *S. aureus* PC1  $\beta$ -lactamase and the various compounds to be computed. The energy values given in Table 1 correspond to the difference between the energy of the optimized complex, and the sum of the energies of the enzyme and the ligand, taken in the conformation they adopt in the complex [37]. With class A  $\beta$ -lactamases, the opening of the  $\beta$ -lactam ring induces no dramatic changes in the relative positions of the various atoms involved in enzyme-substrate binding [37,39–41]. Hence, for a given compound, the three components of the total energy of interaction associated with the formation of the Henri-Michaelis complex, i.e. van der Waals, electrostatic and hydrogen bond, should not differ significantly between ES and ES\*, while the contribution

of the covalent bond is most likely independent on the structure of the substrate. Thus, although the total energies of interaction at the level of the acyl-enzymes are certainly different from those shown in Table 1, the ranking of the different compounds should not be markedly different. With cefazolin and cephaloglycin, calculations were also performed in the absence of the respective side-chains on C-3'. In both cases, the interaction energies of the leaving groups (25 kJ/mol and 23 kJ/mol for cefazolin and cephaloglycin, respectively), not present in the acyl-enzyme, with the enzyme in the corresponding Henri-Michaelis complexes are negligible (178 kJ/mol and 231 kJ/mol for cefazolin and cephaloglycin, respectively).

There appears to be a good correlation between the extent of stabilization observed with the different substrates, and the magnitude of the corresponding energies of interaction with the enzyme. As indicated by the dashed line in Table 1, two groups of substrates can be clearly distinguished. Thus, with the three less effective compounds (cefazolin, 6-aminopenicillanic acid and penicillanic acid), the half-life ( $t_{1/2}$ ) of the inactivation process at 50°C is enhanced by a factor of  $\sim 4$ , and energy values in the range of 150–180 kJ mol<sup>-1</sup> were calculated. By contrast, significantly higher values (210–270 kJ mol<sup>-1</sup>) were obtained with ampicillin, nitrocefin, cephaloglycin and benzylpenicillin, which are much better stabilizing agents ( $t_{1/2}$  at 50°C is enhanced by a factor >40).

Interestingly, Rahil and Pratt [42] showed that the *S. aureus* PC1  $\beta$ -lactamase was significantly stabilized by covalently bound transition-state analog inhibitors. The results obtained here indicate, at least qualitatively, a similar effect with good substrates.

### 3. Significance

Although enzyme stabilization or destabilization upon ligand binding is a well-known phenomenon, quantitative data about the influence of substrates are relatively scarce, because their concentration is due to change during the course of measurement. Here, we were able to monitor the thermal inactivation of the *S. aureus* PC1  $\beta$ -lactamase by directly following the decrease of the rate of substrate utilization. Not unexpectedly, substrate concentrations well below the  $K_m$  value have no stabilizing effect, but protection increases with substrate concentration and reaches a maximum under saturating conditions.

A model was used to simulate the kinetic traces obtained for the hydrolysis of cefazolin at 52°C. The simulations account for the experimental results in a satisfactory manner, and the constants which could not be directly determined (i.e. those characterizing the denaturation rate of the Henri-Michaelis complex and of the acyl-enzyme adduct) can be assigned values within a rather wide variation range without affecting significantly the simulation. The efficiency of the protection is strongly

substrate-dependent and correlates well with the calculated energies of interaction of the various Henri–Michaelis complexes, which also appear to be valid for the corresponding covalent species. This is consistent with the view [8,42–43] that the difference in stability between the free enzyme and the saturated ligand–enzyme complex quantitatively measures the non-covalent energetic complementarity between the ligand and the enzyme.

## 4. Materials and methods

### 4.1. Enzymes and chemicals

The *S. albus* G ( $M_r = 29\,500$ )  $\beta$ -lactamase preparation was that used for the study of the substrate profile [44], and the *S. aureus* PC1 ( $M_r = 28\,800$ ) enzyme was kindly given by Dr R. Virden (University of Newcastle upon Tyne, UK).  $\beta$ -Lactamase concentrations were determined using molecular extinction coefficients of  $32\,750$  and  $19\,870\text{ M}^{-1}\text{ cm}^{-1}$  at  $280\text{ nm}$ , for the *S. albus* G (A. Matagne and J.M. Frère, unpublished data) and the *S. aureus* PC1 [45] enzymes, respectively. Benzylpenicillin was from Rhône-Poulenc (Paris, France), ampicillin was from Bristol Benelux (Brussels, Belgium), 6-aminopenicillanic acid was from Beecham Research Laboratories (Brentford, UK), cefazolin, cephaloglycin and cephalosporin C were from Eli Lilly and Co. (Indianapolis, IN, USA). Penicillanic acid was a gift from Professor P. Claes and the late Professor H. Vanderhaeghe (Katholieke Universiteit, Leuven, Belgium). Nitrocefin was purchased from Oxoid (Basingstoke, UK).

All experiments were performed in  $50\text{ mM}$  sodium phosphate buffer, pH 7, with the addition of  $5\%$  glycerol and  $5\%$  ethylene glycol in the case of the *S. albus* G  $\beta$ -lactamase. Buffer solutions containing  $0.1\text{ mg ml}^{-1}$  of bovine serum albumin (BSA) were used to dilute this enzyme below a concentration of  $0.1\text{ mg ml}^{-1}$ . BSA  $0.1\text{ mg ml}^{-1}$  was also used in the stopped-flow kinetic experiments performed with the *S. aureus* PC1  $\beta$ -lactamase. With both enzymes, the presence of BSA was shown not to influence the kinetics (thermal inactivation and acyl–enzyme formation, respectively).

### 4.2. Equilibrium unfolding transitions (*S. aureus* PC1)

Thermal unfolding curves of the free enzyme were obtained by intrinsic fluorescence and catalytic activity measurements. Fluorescence measurements were performed on a Perkin-Elmer LS50 spectrofluorimeter, with excitation and emission wavelengths of  $280\text{ nm}$  and  $335\text{ nm}$ , respectively, and using a protein concentration of  $\sim 0.07\text{ mg ml}^{-1}$  ( $2.4\text{ }\mu\text{M}$ ). Enzyme activity was followed by absorbance measurements on a UVIKON 860 spectrophotometer (Kontron Instrument). The enzyme was incubated at various temperatures from  $20^\circ\text{C}$  to  $60^\circ\text{C}$ , using an enzyme concentration of  $\sim 0.025\text{ mg ml}^{-1}$  ( $0.9\text{ }\mu\text{M}$ ). Samples were withdrawn at regular time intervals, and the initial rate of  $1\text{ mM}$  benzylpenicillin hydrolysis ( $\Delta\epsilon_M = -775\text{ M}^{-1}\text{ cm}^{-1}$  at  $235\text{ nm}$ ) was rapidly determined at  $30^\circ\text{C}$ , before any significant refolding could take place. The observation of a time-independent initial rate indicated that equilibrium had been reached.

The equilibrium thermal unfolding curves obtained by both

methods were analyzed by assuming a two-state transition, and the data were fitted using Eq. 5 [20]

$$y = \{(N + pT) + (U + qT) \times \exp(a)\} / \{1 + \exp(a)\} \quad (5)$$

with  $a = \Delta H_m \times [(T/T_m) - 1] / RT$

where  $T_m$  is the mid-point of the thermal unfolding curve,  $T_m = T$  at  $\Delta G = 0$ , and  $\Delta H_m$  is the enthalpy of unfolding at  $T_m$ .

### 4.3. Unfolding kinetics

Denaturation rate constants ( $k_u$ ) were derived by fitting the kinetic traces to single exponential functions. In the absence of substrate, the kinetics of thermal unfolding of the free *S. aureus* PC1 enzyme ( $0.07\text{ mg ml}^{-1}$ ) were followed by the decrease in fluorescence emission at  $335\text{ nm}$ , with excitation at  $280\text{ nm}$ . The thermal stability of the *S. albus* G  $\beta$ -lactamase was assayed as described in [44].

In the presence of substrate, enzyme inactivation was followed by monitoring the hydrolysis of the substrate, and using Eq. 6 [46]

$$(v_t - v_{ss}) / (v_0 - v_{ss}) = \exp(-k_u \times t) \quad (6)$$

where  $v_t$  and  $v_0$  are the rate of transformation of the reporter substrate at times  $t$  and  $0$ , respectively, and  $v_{ss}$  is the rate of transformation at the steady-state. Concentrations in the range of  $0.01$ – $100\text{ }\mu\text{g ml}^{-1}$  ( $0.35$ – $350\text{ nM}$ ), and  $0.02$ – $2\text{ }\mu\text{g ml}^{-1}$  ( $0.7$ – $70\text{ nM}$ ) were used for the *S. aureus* PC1 and the *S. albus* G enzymes, respectively, depending on both the temperature and the substrate.

At non-saturating substrate concentrations, a correction was introduced to account for the decrease in rate due to substrate utilization during the inactivation reaction [46].

### 4.4. Determination of the kinetic parameters (*S. aureus* PC1)

In general, a complete time-course of the hydrolysis of the substrate was recorded and the steady-state parameters ( $k_{cat}$  and  $K_m$ ) were derived as described in [46]. At the highest temperatures ( $40^\circ\text{C}$  and  $48^\circ\text{C}$ ), however, enzyme inactivation is not negligible over the experiment time scale, and initial rates were determined and fitted to the Henri–Michaelis equation. In all experiments,  $k_{cat}$  values were also derived from initial rate measurements at saturating substrate concentrations.

### 4.5. Determination of the first-order rate constant ( $k_2$ ) for acylation (*S. aureus* PC1)

Using cefazolin as a substrate, acyl–enzyme formation was directly monitored at  $263\text{ nm}$ , in the temperature range from  $15^\circ\text{C}$  to  $30^\circ\text{C}$ . These experiments were carried out using a Bio-logic SFM-3 stopped-flow apparatus. In all experiments, cefazolin ( $6$ – $70\text{ }\mu\text{M}$ ) was mixed with  $5\text{ }\mu\text{M}$  enzyme and the kinetic data fitted to:

$$A_{263} = B \times \exp(-k_a t) + vt \quad (7)$$

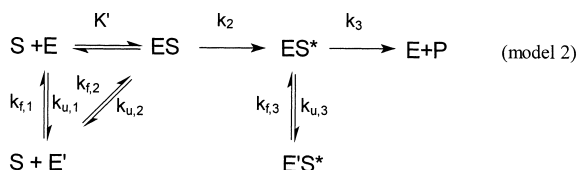
where  $A_{263}$  is the absorbance at  $263\text{ nm}$ ,  $B$  is the size of the ‘burst’,  $k_a$  is the pseudo first-order rate constant for acyl–enzyme formation, and  $v$  is the rate of cefazolin hydrolysis when the steady-state has been reached. Under these conditions and on the basis of model 1, the dependence of  $k_a$  on the concentration

of substrate is given by Eq. 8:

$$k_a = k_3 + (k_2 \times [S]) / (K' + [S]) \quad (8)$$

#### 4.6. Analysis of the unfolding kinetics (*S. aureus* PC1)

The following model was used to account for the influence of substrate on the  $k_u$  value:



Under the experimental conditions where the influence of the substrate concentration on thermal unfolding was analyzed in detail, it could be considered that the steady-state was reached in the catalytic branch (model 2) within the manual mixing dead-time. Indeed, even at the lowest substrate concentration, the turnover number remained larger than  $1 \text{ s}^{-1}$ , while the  $k_{u,1}$  value is less than  $0.1 \text{ s}^{-1}$ . Hence, the time-courses of the product (P), the native ( $E + ES + ES^*$ ) and the denatured ( $E'$  and  $E'S^*$ ) enzyme species are given by:

$$\frac{dx}{dt} = Dy + Fz - Ax \quad (9)$$

$$\frac{dy}{dt} = (A - B)x - Dy \quad (10)$$

$$\frac{dz}{dt} = Bx - Fz \quad (11)$$

$$\frac{dP}{dt} = Gx \quad (12)$$

where:

$$x = [E] + [ES] + [ES^*], \quad y = [E'], \quad z = [E'S^*]$$

and:

$$A = [(k_{u,1} \times k_3 \times K') + (k_{u,2} \times k_3 \times [S]) +$$

$$(k_{u,3} \times k_2 \times [S])] / [(k_3 \times K') + (k_2 + k_3) \times [S]] \quad (13)$$

$$B = (k_{u,3} \times k_2 \times [S]) / [(k_3 \times K') + (k_2 + k_3) \times [S]] \quad (14)$$

$$D = k_{f,1} + (k_{f,2} \times [S]) \quad (15)$$

$$F = k_{f,3} \quad (16)$$

$$G = (k_{cat} \times [S]) / (K_m + [S]) \quad (17)$$

The program GraFit 3.09 (Erithacus software) was used to carry out linear or non-linear least-squares fitting of the data. Simulations were performed with the help of the Berkeley-Madonna 7.0.1. software (Kagi Shareware, Berkeley, CA, USA).

#### 4.7. Molecular modelling

The crystallographic structure from the Brookhaven Protein Data Bank (entry 3BLM) was used for the *S. aureus* PC1  $\beta$ -lactamase [47].

The structures of the  $\beta$ -lactam compounds were optimized by the AM1 semi-empirical method, with the Ampac/Mopac module

of the INSIGHT II package (Molecular Simulations, Inc., San Diego, CA, USA).

Each antibiotic structure was docked into the enzyme active site, and the geometry of the corresponding Henri-Michaelis complexes was optimized by total energy minimization with the use of the molecular mechanics AMBER V 4.1 framework [48], running on a Silicon Graphics Indy workstation. Standard point charges on the amino acid residues and a distance-dependent dielectric constant,  $\epsilon = R_{ij}$ , were used for the calculation of the Coulombic term. CH, CH<sub>2</sub> and CH<sub>3</sub> groups were treated as united atoms. CNDO partial atomic charges on the ligands were used. The bond lengths, angles, and ring dihedral angles of the substrates were constrained to the AM1 values, while allowing rotation around the free bonds, as described in [37].

#### Acknowledgements

This work was supported by the Belgian Government in the frame of the Pôles d'Attraction Interuniversitaires (PAI P4/03). M.V. and A.M. are Postdoctoral Researcher and Research Associate, respectively, of the National Fund for Scientific Research (F.N.R.S., Belgium). A.L. was the recipient of a F.R.I.A. fellowship (F.N.R.S., Belgium).

#### References

- [1] N. Citri, N. Zyk, The interaction of penicillinase with penicillins. IV. Structural aspects of catalytic and non-catalytic interactions, *Biochim. Biophys. Acta* 99 (1965) 427–441.
- [2] C. Frömmel, W.E. Höhne, Influence of calcium binding on the thermal stability of 'thermitase', a serine protease from *Thermoactinomyces vulgaris*, *Biochim. Biophys. Acta* 670 (1981) 25–31.
- [3] R. Griebler, S. D'Auria, F. Tanfani, B. Nidetzky, Thermal denaturation pathway of starch phosphorylase from *Corynebacterium callunae*: oxyanion binding provides the glue that efficiently stabilizes the dimer structure of the protein, *Protein Sci.* 9 (2000) 1149–1161.
- [4] I. Villaume, D. Thomas, M.D. Legoy, Catalysis may increase the stability of an enzyme: the example of horse liver alcohol dehydrogenase, *Enzyme Microb. Technol.* 12 (1990) 506–509.
- [5] S. Nakamura, K. Koga, Alteration of thermal stability of glucose oxidase associated with the redox states, *Biochem. Biophys. Res. Commun.* 78 (1977) 806–810.
- [6] S. Kanaya, M. Oobatake, Y. Liu, Thermal stability of *Escherichia coli* ribonuclease HI and its active site mutants in the presence and absence of the Mg<sup>2+</sup> ion. Proposal of a novel catalytic role for Glu-48, *J. Biol. Chem.* 271 (1996) 32729–32736.
- [7] D.J. Sharpe, L.J.C. Wong, Effects of substrates on the thermal stability of nuclear histone acetyltransferase, *Biochimie* 72 (1990) 323–326.
- [8] B.M. Beadle, S.L. McGovern, A. Patera, B.K. Shoichet, Functional analyses of AmpC  $\beta$ -lactamase through differential stability, *Protein Sci.* 8 (1999) 1816–1824.
- [9] K. Burton, The stabilization of D-amino acid oxidase by flavin-adenine dinucleotide, substrates and competitive inhibitors, *Biochem. J.* 48 (1951) 458–467.
- [10] J. Südi, Kinetics of the protection of lactate dehydrogenase by substrates against heat inactivation, *Biochim. Biophys. Acta* 212 (1970) 213–224.
- [11] C.N. Pace, T. Mc Grath, Substrate stabilization of lysozyme to ther-

- mal and guanidine hydrochloride denaturation, *J. Biol. Chem.* 255 (1980) 3862–3865.
- [12] S.G. Waley,  $\beta$ -Lactamase: mechanism of action, in: M.I. Page (Ed.), *The Chemistry of  $\beta$ -Lactams*, Blackie, London, 1992, pp. 198–228.
  - [13] A. Matagne, A. Dubus, M. Galleni, J.M. Frère, The  $\beta$ -lactamase cycle: a tale of selective pressure and bacterial ingenuity, *Nat. Prod. Rep.* 16 (1999) 1–19.
  - [14] H. Christensen, M.T. Martin, S.G. Waley,  $\beta$ -Lactamases as fully efficient enzymes. Determination of all the rate constants in the acyl-enzyme mechanism, *Biochem. J.* 266 (1990) 853–861.
  - [15] W.S. Faraci, R.F. Pratt, Mechanism of inhibition of the PC1  $\beta$ -lactamase of *Staphylococcus aureus* by cephalosporins: importance of the 3'-leaving group, *Biochemistry* 24 (1985) 903–910.
  - [16] B. Robson, R.H. Pain, The mechanism of folding of globular proteins. Equilibria and kinetics of conformational transitions of penicillinase from *Staphylococcus aureus* involving a state of intermediate conformation, *Biochem. J.* 155 (1976) 331–344.
  - [17] S. Craig, M. Hollecker, T.E. Creighton, R.H. Pain, Single amino acid mutations block a late step in the folding of  $\beta$ -lactamase from *Staphylococcus aureus*, *J. Mol. Biol.* 185 (1985) 681–687.
  - [18] V.N. Uversky, O.B. Ptitsyn, 'Partly folded' state. A new equilibrium state of protein molecules: four-state guanidinium chloride-induced unfolding of  $\beta$ -lactamase at low temperature, *Biochemistry* 33 (1994) 2782–2791.
  - [19] K.A. Wheeler, A.R. Hawkins, R. Pain, R. Virden, The slow step of folding of *Staphylococcus aureus* PC1  $\beta$ -lactamase involves the collapse of a surface loop rate limited by the *trans* to *cis* isomerization of a non-proline peptide bond, *Proteins* 33 (1998) 550–557.
  - [20] M. Vanhove, S. Houba, J. Lamotte-Brasseur, J.M. Frère, Probing the determinants of protein stability: comparison of class A  $\beta$ -lactamases, *Biochem. J.* 308 (1995) 859–864.
  - [21] C.N. Pace, J.M. Scholtz, Measuring the conformational stability of a protein, in: T.E. Creighton (Ed.), *Protein Structure, a Practical Approach*, 2nd edn., Oxford University Press, Oxford, 1997, pp. 299–321.
  - [22] B.L. Chen, W.A. Baase, J.A. Schellman, Low-temperature unfolding of a mutant of phage T4 lysozyme. 2. Kinetic investigations, *Biochemistry* 28 (1989) 691–699.
  - [23] M. Oliveberg, Y.J. Tan, A.R. Fersht, Negative activation enthalpies in the kinetics of protein folding, *Proc. Natl. Acad. Sci. USA* 92 (1995) 8926–8929.
  - [24] T. Schindler, F.X. Schmid, Thermodynamic properties of an extremely rapid protein folding reaction, *Biochemistry* 35 (1996) 16833–16842.
  - [25] M.L. Scalley, D. Baker, Protein folding kinetics exhibit an Arrhenius temperature dependence when corrected for the temperature dependence of protein stability, *Proc. Natl. Acad. Sci. USA* 94 (1997) 10636–10640.
  - [26] A. Matagne, M. Jamin, E.W. Chung, C.V. Robinson, S.E. Radford, C.M. Dobson, Thermal unfolding of an intermediate is associated with non-Arrhenius kinetics in the folding of hen lysozyme, *J. Mol. Biol.* 297 (2000) 193–210.
  - [27] A.R. Fersht, Characterizing transition states in protein folding: an essential step in the puzzle, *Curr. Opin. Struct. Biol.* 5 (1995) 79–84.
  - [28] L.S. Itzhaki, D.E. Otzen, A.R. Fersht, The structure of the transition state for folding of chymotrypsin inhibitor 2 analysed by protein engineering methods: evidence for a nucleation-condensation mechanism for protein folding, *J. Mol. Biol.* 254 (1995) 260–288.
  - [29] M.E. Milla, B.M. Brown, C.D. Waldburger, R.T. Sauer, P22 Arc repressor: transition state properties inferred from mutational effects on the rates of protein unfolding and refolding, *Biochemistry* 34 (1995) 13914–13919.
  - [30] G.J. Vidugiris, J.L. Markley, C.A. Royer, Evidence for a molten globule-like transition state in protein folding from determination of activation volumes, *Biochemistry* 34 (1995) 4909–4912.
  - [31] Y.J. Tan, Y.J. Oliveberg, A.R. Fersht, Titration properties and thermodynamics of the transition state for folding: comparison of two-state and multi-state folding pathways, *J. Mol. Biol.* 264 (1996) 377–389.
  - [32] K.W. Plaxco, J.I. Guijarro, C.J. Morton, M. Pitkeathly, I.D. Campbell, C.M. Dobson, The folding kinetics and thermodynamics of the Fyn-SH3 domain, *Biochemistry* 37 (1998) 2529–2537.
  - [33] E.R. Main, K.F. Fulton, S.E. Jackson, Folding pathway of FKBP12 and characterisation of the transition state, *J. Mol. Biol.* 291 (1999) 429–444.
  - [34] S.I. Segawa, M. Sugihara, Characterization of the transition state of lysozyme unfolding. I. Effect of protein-solvent interactions on the transition state, *Biopolymers* 23 (1984) 2473–2488.
  - [35] S.E. Jackson, A.R. Fersht, Folding of chymotrypsin inhibitor 2. 2. Influence of proline isomerization on the folding kinetics and thermodynamic characterization of the transition state of folding, *Biochemistry* 30 (1992) 10436–10443.
  - [36] P. Alexander, J. Orban, P. Bryan, Kinetic analysis of folding and unfolding the 56 amino acid IgG-binding domain of streptococcal protein G, *Biochemistry* 31 (1992) 7243–7248.
  - [37] J. Lamotte-Brasseur, G. Dive, O. Dideberg, P. Charlier, J.M. Frère, J.M. Ghuysen, Mechanism of acyl transfer by the class A serine  $\beta$ -lactamase of *Streptomyces albus* G, *Biochem. J.* 279 (1991) 213–221.
  - [38] J. Lamotte-Brasseur, V. Lounnas, X. Raquet, R.C. Wade,  $pK_a$  calculations for class A  $\beta$ -lactamases: influence of substrate binding, *Protein Sci.* 8 (1999) 404–409.
  - [39] O. Herzberg, J. Moult, Bacterial resistance to  $\beta$ -lactam antibiotics: crystal structure of  $\beta$ -lactamase from *Staphylococcus aureus* PC1 at 2.5 Å resolution, *Science* 236 (1987) 694–701.
  - [40] P.C. Moews, J.R. Knox, O. Dideberg, P. Charlier, J.M. Frère,  $\beta$ -Lactamase of *Bacillus licheniformis* 749/C at 2 Å resolution, *Proteins Struct. Funct. Genet.* 7 (1990) 156–171.
  - [41] N.C.J. Strynadka, H. Adachi, S.E. Jensen, K. Johns, A. Sielecki, C. Betzel, K. Sutoh, M.N.J. James, Molecular structure of the acyl-enzyme intermediate in  $\beta$ -lactam hydrolysis at 1.7 Å resolution, *Nature* 359 (1992) 700–705.
  - [42] J. Rahil, R.F. Pratt, Characterization of covalently bound enzyme inhibitors as transition-state analogs by protein stability measurements: phosphonate monoester inhibitors of a  $\beta$ -lactamase, *Biochemistry* 33 (1994) 116–125.
  - [43] A. Morton, B.W. Matthews, Specificity of ligand binding in a buried nonpolar cavity of T4 lysozyme: linkage of dynamics and structural plasticity, *Biochemistry* 34 (1995) 8576–8588.
  - [44] A. Matagne, A.M. Misselyn-Bauduin, B. Joris, T. Erpicum, B. Granier, J.M. Frère, The diversity of the catalytic properties of class A  $\beta$ -lactamases, *Biochem. J.* 265 (1990) 131–146.
  - [45] C. Mitchinson, R.H. Pain, Effects of sulphate and urea on the stability and reversible unfolding of  $\beta$ -lactamase from *Staphylococcus aureus*. Implications for the folding pathway of  $\beta$ -lactamase, *J. Mol. Biol.* 184 (1985) 331–342.
  - [46] F. De Meester, B. Joris, G. Reckinger, C. Bellefroid-Bourguignon, J.M. Frère, S.G. Waley, Automated analysis of enzyme inactivation phenomena. Application to  $\beta$ -lactamases and DD-peptidases, *Biochem. Pharmacol.* 36 (1987) 2393–2403.
  - [47] O. Herzberg, Refined crystal structure of  $\beta$ -lactamase from *Staphylococcus aureus* PC1 at 2.0 Å resolution, *J. Mol. Biol.* 217 (1991) 701–719.
  - [48] D. Pearlman, D.A. Case, J.A. Caldwell, W.S. Ross, T.E. Cheatham, D.M. Ferguson, G.L. Seibel, U.C. Singh, P.K. Weiner, P.A. Kollman, AMBER 4.1. University of California, San Francisco, CA, 1995.